International Journal of Industrial Engineering & Management Science, Vol. 9, Issue 1, (2022) 35-43

University of Hormozgan

International Journal of Industrial Engineering & Management Science

journal homepage: www.ijiems.com

An Analysis on Boundary Layer Flows over a Vertical Slender Cylinder Via Spectral Method

Mehran Nikarya [a,*]

[a] Department of Electrical Engineering and Information Technology Iranian Research Organization for Science and Technology(IROST), Tehran, Iran

A R T I C L E I N F O

Article history:
Received: 2022-03-05
Received in revised form: -
Accepted: 2022-06-01

Keywords:
Vertical slender cylinder
Boundary layer
Suction/injection
Spectral collocation method
Bessel functions of the first kind

A B S T R A C T

In this research, an analysis is carried out to study the effects that blowing/injection and suction on the steady mixed convection or combined forced and free convection boundary layer flows over a vertical slender cylinder with a mainstream velocity and a wall surface temperature proportional to the axial distance along the surface of the cylinder. To study the problem, the non-linear partial differential equations and their associated boundary conditions are transformed into coupled non-linear ordinary differential equations. In this paper, we have solved this equation by a newly developed spectral collocation method based on Bessel functions of the first kind and also to compare the skin friction, we used the shooting method. After solving the problem, we have discussed about the values of the skin friction coefficient, the local Nusselt number, curvature parameter, buoyancy or mixed convection parameter and Prandtl number. Also, a comparison is made with the corresponding results to show reliability of presented method.

1. Introduction

Recently, the mixed convection flows, combined forced and free convection flows occur in many transport processes of natural and engineering devices, such as, nuclear reactors cooled during emergency shutdown, heat exchangers placed in a low velocity environment, etc. [1, 2, 3]. Such a process occurs when the effect of the buoyancy force in forced convection or the effect of forced flow in free convection becomes significant. The effect is especially pronounced in situations where the forced flow velocity is low and the temperature difference is large [4]. Mixed convection flow of a viscous and incompressible fluid over various geometries, such as, flat plates, moving sheets, cylinders and spheres has been performed and correlations obtained for each one. Kumari and Nath [1, 5] studied the effects of localized cooling/heating and injection/suction on the mixed convection flow on a thin vertical cylinder. Aydin and Kaya [6] numerically studied the problem of steady laminar magneto hydrodynamic (MHD) mixed convection heat transfer about a vertical slender cylinder. Kuiken [7] investigated radial curvature effects on axisymmetric free convection boundary layer flow for vertical cylinders and cones for some special non-uniform temperature differences between the surface and the ambient fluid. Lok et al. [8] studied the unsteady mixed convection boundary-layer flow of a micropolar fluid near the region of the stagnation point on a double-infinite vertical flat plate. Hassanien and Gorla [9] presented boundary layer solutions to study the effects of buoyancy on forced convective micropolar fluid flow and heat transfer in stagnation flows using the theory of micropolar fluids formulated by Eringen. Ishak et al. [10] analyzed theoretically (numerically) the effects that blowing/injection and suction have on the steady mixed convection or combined forced and free convection boundary layer flows over a vertical slender cylinder with a mainstream velocity and a wall surface temperature

* Corresponding author.
E-mail address: mehran.nikarya@gmail.com

proportional to the axial distance along the surface of the cylinder. The fundamental governing equations for fluid mechanics are the Navier-Stokes equations [11, 12, 13]. This inherently non-linear set of partial differential equations has no general solution, and only a small number of exact solutions have been found (see [14]). The importance of exact solutions is because the solutions represent fundamental fluid-dynamic flows and also owing to the uniform validity of exact solutions, the basic phenomena described by the Navier-Stokes equations can be studied more closely, and they act as standards for checking the accuracies of many approximate methods, whether they are numerical, asymptotic, or empirical. Explicit solutions are used as models for physical or numerical experiments, and often reflect the asymptotic behavior of more complicated solutions. All explicit solutions for the boundary layer equations are seemingly similar solutions in the sense that the longitudinal velocity component displays the same shape of profile across any transverse section of the layer, see Schlichting [15].

Spectral methods, in the context of numerical schemes for differential equations, generically belong to the family of weighted residual methods (WRMs)[16]. WRMs represent a particular group of approximation techniques, in which the residuals (or errors) are minimized in a certain way and thereby leading to specific methods including Galerkin, Petrov-Galerkin, collocation and tau formulations. WRMs are traditionally regarded as the foundation and cornerstone of the finite element, spectral, finite volume, boundary element and some other methods [16]. The key components of their formulation are the trial functions and the test functions. The trial functions, which are the linear combinations of suitable trial basis functions, are used to provide an approximate representation of the solution. The test functions are used to ensure that the differential equation and perhaps some boundary conditions are satisfied as closely as possible by the truncated series expansion. This is achieved by minimizing the residual function that is produced by using the truncated expansion instead of the exact solution with respect to a suitable norm [16,17,18].

In this paper, we attempt to use the Bessel functions of the first kind as basic functions for spectral-collocation method for solving a set of non-linear ordinary differential equations (ODE) with boundary conditions in the infinite. In the past, the Bessel functions collocation and Bessel polynomials collocation methods have been used for solving some problems, for example see [19, 20, 21, 22], but now, we aim to use BFC method for solving set of ODE with conditions in the infinite.

The rest of this paper is organized as follows: In Section 2, we describe the formulation of equations. In Section 3 the Bessel functions of the first kind is explained. In Section 4, we describe the function approximation and our proposed method. In Section 4.1, by applying the proposed method for solving the vertical slender cylinder equations. Finally, in the last section, we have described the concluding remarks.

2. Formulation of Equations

Let us consider a thin vertical circular cylinder of radius R with wall surface temperature proportional to the axial distance along the surface of the cylinder. Let U_∞ and T_∞ be velocity and temperature in the free stream, respectively. Fig. 1 illustrates the physical model and coordinate system. r shows the radial coordinate that is measured from the axis of cylinder and the axial coordinate x is measured vertically upwards such that $x = 0$ corresponds to the leading edge, where the boundary layer thickness is zero, the fluid properties are assumed to be constant except the density changes which giving arise to the buoyancy forces. The viscous dissipation has been neglected in the energy equation. It is assumed that the injected fluid possesses the same physical properties as a boundary layer fluid and has a static temperature equal to the wall temperature. Under the above assumptions and taking into account the Boussinesq approximation equations of continuity, momentum and energy under boundary layer approximations governing the mixed convection flow over a thin vertical cylinder can be expressed as [23]

$$\frac{\partial}{\partial x}(ru) + \frac{\partial}{\partial r}(rw) = 0\,, \tag{1}$$

$$u\frac{\partial u}{\partial x} + w\frac{\partial u}{\partial r} = U\frac{dU}{dx} + \nu\left(\frac{\partial^2 u}{\partial r^2} + \frac{1}{r}\frac{\partial u}{\partial r}\right) + g\beta(T - T_\infty)\,, \tag{2}$$

$$u\frac{\partial T}{\partial x} + w\frac{\partial T}{\partial r} = \alpha\left(\frac{\partial^2 T}{\partial r^2} + \frac{1}{r}\frac{\partial T}{\partial r}\right), \tag{3}$$

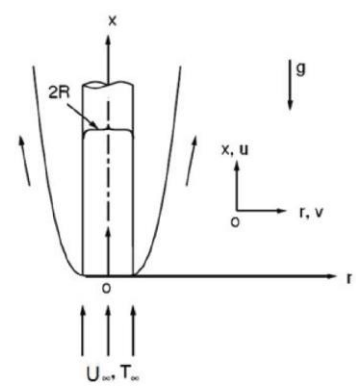

Figure 1. Physical model and coordinate system

where $U(x)$ is the mainstream velocity, r and x are distances along the radial and axial directions, respectively, u and w are the velocity components along x and r directions, respectively, T is the temperature, g is the magnitude of the acceleration due to gravity, β is the volumetric coefficient of thermal expansion, α is the thermal diffusivity and ν the kinematic viscosity. Assuming that the appropriate boundary conditions are:

$$\begin{array}{llll} u = 0 & w = V & T = T_w & at \quad r = R \\ u \to U(x) & T \to T_\infty & & at \quad r \to \infty \end{array} \tag{4}$$

where V is the constant velocity of injection $(V > 0)$ or suction $(V < 0)$. Further, we assume that the mainstream velocity $U(x)$ and the temperature of the cylinder surface $T_w(x)$ have the form

$$U(x) = U_\infty\left(\frac{x}{l}\right), \quad T_w(x) = T_\infty + \Delta T\left(\frac{x}{l},\right)$$

where l is a characteristic length, U_∞ is the characteristic velocity and $\triangle T$ is the characteristic temperature with $\triangle T > 0$ for a heated surface and $\triangle T < 0$ for a cooled surface. Ishak et al. [10] by using the similarity transformation reduced the above equations to a set of nonlinear ordinary differential equations. They introduced the similarity variables as follow

$$\eta = \frac{r^2-R^2}{2R}\sqrt{\frac{U}{\nu x}}, \quad \psi = \sqrt{U\nu x}Rf(\eta),$$
$$\theta(\eta) = \frac{T-T_\infty}{T_w-T_\infty} \tag{5}$$

where ψ is the stream function defined as $u = r^{-1}\partial\psi/\partial r$ and $w = -r^{-1}\partial\psi/\partial x$, which identically satisfy Eq. (1). By using this definition, we obtain

$$u = Uf'(\eta), \quad w = -\frac{R}{r}\sqrt{\frac{\nu U_\infty}{l}}f(\eta),$$

where primes denote differentiation with respect to η. In order that similarity solutions exist, V has to be of the form

$$V = -\frac{R}{r}\sqrt{\frac{\nu U_\infty}{l}}f_0$$

where $f_0 = f(0)$ and $f_0 < 0$ is for mass injection and $f_0 > 0$ is for mass suction. Substituting Eq. (5) into Eqs. (2) and (3), we can get the following ordinary differential equations

$$(1+2\gamma\eta)f''' + 2\gamma f'' + ff'' + 1 - (f')^2 + \lambda\theta = 0\,,$$
$$(1+2\gamma\eta)\theta'' + 2\gamma\theta' + Pr(f\theta' - f'\theta) = 0\,, \tag{6}$$

subject to the boundary conditions (4) which become

$$f(0) = f_0, \quad f'(0) = 0, \quad f'(\infty) = 1$$
$$\theta(0) = 1, \quad \theta(\infty) = 0, \tag{7}$$

where γ is the curvature parameter and λ is the buoyancy or mixed convection parameter defined as

$$\gamma = \sqrt{\frac{\nu l}{U_\infty R^2}} \quad , \quad \lambda = \frac{g\beta l\triangle T}{U_\infty^2} \tag{8}$$

respectively. In Eq. (8), $\lambda > 0$ and $\lambda < 0$ correspond to the aiding flow (heated cylinder) and to the opposing flow (cooled cylinder), respectively, while $\lambda = 0$ represents the pure forced convection flow (buoyancy force is absent). It is worth mentioning that the similarity solution of Eqs. (6) and (7) is not necessarily the only solution to the problem as the governing equations are non-linear. We notice that when $\gamma = 0$ (i.e. $R \to \infty$), the problem under consideration reduces to the flat plate case considered by Ishak et al. [24], while when $f_0 = 0$, it reduces to the impermeable cylinder considered by Mahmood and Merkin [25]. Furthermore, when both γ and and f_0 are zero, the present problem reduces to the problem considered by Ramachandran et al. [26] for the case of an arbitrary surface temperature with $n = 1$ in their paper. The physical quantities of interest are the skin friction coefficient C_f and the local Nusselt number Nu_x, which are defined by

$$C_f = \frac{2\tau_w}{\rho U^2}\,, \quad Nu_x = \frac{xq_w}{k(T_w - T_\infty)},$$

where τ is the skin friction and q_w is the heat transfer from plate and given by

$$\tau_w = \mu(\frac{\partial u}{\partial r})_{r=R} \quad , \quad q_w = -k(\frac{\partial T}{\partial r})_{r=R}$$

where μ is the dynamic viscosity and k is the thermal conductivity. Using the similarity variables (5), we get

$$\frac{1}{2}C_f Re_x^{\frac{1}{2}} = f''(0) \;\; , \;\; \frac{Nu_x}{Ru_x^{\frac{1}{2}}} = -\theta'(0),$$

where $Re_x = Ux/\nu$ is the local Reynolds number.

3. Bessel Functions of the First Kind

The Bessel's equation of order n, is [27, 28]:

$$x^2y''(x) + xy'(x) + (x^2 - n^2)y(x) = 0,$$
$$\text{for } x \in (-\infty, \infty), \;\; (n \in \mathbb{R}). \tag{9}$$

An obtained solution of this equation is [28]:

$$\sum_{r=0}^{\infty} a_0 \frac{(-1)^r\Gamma(n+1)}{2^{2r}r!\,\Gamma(n+r+1)}(\frac{x}{2})^{2r+n},$$

for any value of a_0; where $\Gamma(\lambda)$ is the gamma function defined as follows:

$$\Gamma(\lambda) = \int_0^\infty e^{-t}t^{\lambda-1}dt.$$

Let us choose $a_0 = \frac{1}{2^n\Gamma(n+1)}$. Accordingly, we obtain the solution which we shall denote by $J_n(x)$ and we call it the Bessel function of the first kind of order n:

$$J_n(x) = \sum_{r=0}^{\infty} \frac{(-1)^r}{r!\Gamma(n+r+1)}(\frac{x}{2})^{2r+n}, \tag{10}$$

where series (10) is convergent for all $-\infty < x < \infty$. Now, we express some properties of the first kind of Bessel functions. Some recursive relations of derivation are as follow [28]:

$$\frac{d}{dx}(x^nJ_n(x)) = x^nJ_{n-1}(x), \tag{11}$$

$$J'_n(x)=J_{n-1}(x)-\frac{n}{x}J_n(x). \quad (12)$$

An important property of the first kind of Bessel functions is converging to zero for $J_n^{(m)}(x)$ when $x\to\infty$ for $n,m=0,1,2,3..$

4. Function Approximation

Suppose that $\mathcal{H}=L^2(\Gamma)$, where $\Gamma=(0,+\infty)$, let $\{J_0(x),J_1(x),\dots,J_n(x)\}\subset\mathcal{H}$ be the set of Bessel functions and suppose that

$$\mathbf{J}=\operatorname{span}\{J_0(x),J_1(x),\dots,J_n(x)\}, \quad (13)$$

Since $\mathcal{H}$ is Hilbert space and $\mathbf{J}$ is the finite-dimensional subspace, $\dim\mathbf{J}=n+1$, so $\mathbf{J}$ is a closed subspace of $\mathcal{H}$, therefore, $\mathbf{J}$ is a complete subspace of $\mathcal{H}$. Let f be an arbitrary element in $\mathcal{H}$, therefore, f has a unique best approximation from $\mathbf{J}$, say $\hat{\jmath}\in\mathbf{J}$, that is

$$\exists\,\hat{\jmath}\in\mathbf{J};\ \forall j\in\mathbf{J},\ \|f-\hat{\jmath}\|\le\|f-j\|, \quad (14)$$
where $\|f\|=<f,f>^{1/2}$ and $<f,g>=\int_{-\infty}^{\infty}f(t)g(t)\,dt$

Definition: (Direct sum ($\oplus$)): A vector space $\mathcal{H}$ is said to be the direct sum of two subspaces Y and Z of $\mathcal{H}$, written $\mathcal{H}=Y\oplus Z$, if each $x\in\mathcal{H}$ has a unique representation $x=y+z$. Then, Z is called an algebraic complement of Y in $\mathcal{H}$ and vice versa, and Y,Z is called a complementary pair of subspaces in $\mathcal{H}$.

Definition: Let $\mathcal{H}$ be an Hilbert space and Y be any closed subspace of $\mathcal{H}$. $Y^{\perp}$ is defined the orthogonal complement, as:

$$Y^{\perp}=\{z\in\mathcal{H}\mid z\perp Y\}. \quad (15)$$

Lemma: Let Y be any closed subspace of a Hilbert space $\mathcal{H}$. Then,

$$\mathcal{H}=Y\oplus Y^{\perp}. \quad (16)$$

Proof. See [29].

Now, by using (13) and (14), we can say $\mathcal{H}=\mathbf{J}\oplus Z$,

where $Z=\mathbf{J}^{\perp}$, so that for each $x\in\mathcal{H}$, $x=j+z$. Where $z=x-j\perp j$, hence, $<x-j,j>=0$. We have $j\in\mathbf{J}$, therefore,

$$j=\sum_{k=0}^{n}a_k\,J_k(x), \quad (17)$$

and $x-j\perp j$ gives the n conditions

$$<J_m(x),x-j>=<J_m(x),x-\sum_{k=0}^{n}a_k\,J_k(x)>=0, \quad (18)$$

that is

$$<J_m(x),x>=\sum_{k=0}^{n}\bar{a}_k\ <J_m(x),J_k(x)>,\quad m=0,1,\dots,n. \quad (19)$$

This is a nonhomogeneous system of $n+1$ linear equations in $n+1$ unknown coefficients $\{\bar{a}_k\}_{k=0}^{n}$ (spectral coefficients). The determinant of the coefficients is

$$G(J_0(x),J_1(x),\dots,J_n(x))=\begin{vmatrix}<J_0(x),J_0(x)> & <J_0(x),J_1(x)> & \dots & <J_0(x),J_n(x)>\\ <J_1(x),J_0(x)> & <J_1(x),J_1(x)> & \dots & <J_1(x),J_n(x)>\\ \vdots & \vdots & \ddots & \vdots\\ <J_n(x),J_0(x)> & <J_n(x),J_1(x)> & \dots & <J_n(x),J_n(x)>\end{vmatrix}.$$

Since $\mathbf{J}$ exists and is unique, that system has a unique solution. Hence, $G(J_0(x),J_1(x),\dots,J_n(x))$ must be different from 0. The determinant $G(J_0(x),J_1(x),\dots,J_n(x))$ is called the Gram determinant of $J_0(x),J_1(x),\dots,J_n(x)$.

Theorem: Suppose that $\mathcal{H}$ is a Hilbert space and Y a closed subspace of $\mathcal{H}$ such that $\dim Y<\infty$ and $\{y_1,y_2,\dots,y_n\}$ is any basis for Y. Let x be an arbitrary element in $\mathcal{H}$ and y_0 be the unique best approximation to x from Y. Then,

$$\|x-y_0\|^2=\frac{G(x,y_1,y_2,\dots,y_n)}{G(y_1,y_2,\dots,y_n)}, \quad (20)$$

Proof. See [29].

To obtain the Spectral coefficients $\{a_i\}_{i=0}^{N}$ in series (17) and an approach of $u(x)$ via (17), we employ the collocation algorithm introduced as follows:

5. Collocation Algorithm for Solving Problem

A method for solving differential equations is the collocation method, that, by substituting the finite series (17) to equations and constructing the residual function(s) and forcing it to zero on collocation point obtains a solution(s) [16, 30, 31, 18]. In all of the spectral methods, the purpose is to finding these coefficients a_i of expand.

In the following algorithm, we solve the equations (6) with their conditions (7):

At the beginning we must satisfy the conditions in the expanding solutions of $f(\eta)$ and $\theta(\eta)$, therefore, according to the properties of the first kind of the Bessel functions:

$$J_n(0)=\begin{cases}1, & n=0\\ 0, & n\ge 1\end{cases} \quad (21)$$

and $\lim_{\eta\to\infty}J_n(\eta)=0$ for all n and also (12) we can satisfy the two conditions of $f(\eta)$ at zero through starting i from 2, and to satisfy $f'(\infty)=1$ we can multiply series to $\frac{a_i\eta^2}{\eta^{\eta}+1}$ and add with $f_0+\frac{\eta^2}{\eta+l}$. Now, for conditions of $\theta(\eta)$, the Bessel functions satisfy them, but the speed of convergent in the infinite to zero is low, therefore, we multiply the series to $exp(-x)$ and for $\theta(0)=1$ add it with $\exp(-\eta)$ we start i from 1, multiply series to $\exp(-\alpha\eta)$ and add with $exp(-\eta)$. In the following algorithm, we solve the equations (6):

BEGIN

1. Construct the following series by using the (17),

$$\widehat{f_N}(\eta) = f_0 + \frac{\eta^2}{\eta+l} + \frac{a_i\eta^2}{\eta^{\eta}+1}\sum_{i=2}^{N} a_i J_i(\eta) \qquad (22)$$

$$\widehat{\theta_N}(\eta) = exp(-\eta)(1 + \sum_{j=1}^{N} b_j J_j(\eta)) \qquad (23)$$

2. Insert the series of previous step to equations (6) and construct the residual functions as follow:

$$\mathcal{R}_1(\eta) = (1+2\gamma\eta)\widehat{f_N}(\eta)''' + 2\gamma\widehat{f_N}(\eta)'' + \widehat{f_N}(\eta)\widehat{f_N}(\eta)'' + 1 - (\widehat{f_N}(\eta)')^2 + \lambda\widehat{\theta_N}(\eta),$$

$$\mathcal{R}_1(\eta) = (1+2\gamma\eta)\widehat{f_N}(\eta)''' + 2\gamma\widehat{f_N}(\eta)'' + \widehat{f_N}(\eta)\widehat{f_N}(\eta)'' + 1 - (\widehat{f_N}(\eta)')^2 + \lambda\widehat{\theta_N}(\eta),$$

Now, we have $2N-1$ unknowns $\{a_n\}_{n=2}^N$ and $\{b_n\}_{n=1}^N$. To obtain these unknown coefficients, we need $2N-1$ equations, thus:

3. By choosing $N-1$ points $\{x_i\}$, $i = 1,\ldots,N-1$, and N points $\{y_i\}$, $i = 1,\ldots,N$ in the domain of the equations (6) as collocation points and substituting them in $\mathcal{R}_1(\eta)$ and $\mathcal{R}_2(\eta)$, respectively, we construct a system containing $2N-1$ equations and $2N-1$ unknowns.

4. By solving the obtained system of equations in step 4, we gain the $a_n, n = 0,1,\ldots,N$.

5. By substituting the obtained values of $\{a_i\}_{i=2}^N$ and $\{b_j\}_{j=1}^N$ in series of step 2, we approach $f(\eta)$ by $\widehat{f_N}(\eta)$ and $\theta(\eta)$ by $\widehat{\theta_N}(\eta)$.

END.

6. Results

In this section, we show the graphical results of the influence of physical parameters on the velocity $f'(\eta)$, the temperature profile $\theta(\eta)$, the skin friction coefficient $\frac{1}{2}C_f {Re_x}^{1/2}$ and the local Nusselt number $Nu - x/{Ru_x}^{1/2}$. Specifically the attention has been focused to the variations of curvature parameter γ, buoyancy or mixed convection parameter λ, Prandtl number Pr and f_0. For this purpose, the figures 2-5 have been presented. Also the variation of the skin friction coefficient $\frac{1}{2}C_f {Re_x}^{1/2}$ and the local Nusselt number $Nu - x/{Ru_x}^{1/2}$ are computed in tables 1 and 2 for sundry parameters Prandtl number Pr. In these tables, the comparison of the present results has been made with the existing numerical results. An agreement between the results is noted in the limiting sense. Figure 3 shows the influence of f_0 on velocity and temperature profiles for two cases of buoyancy or mixed convection parameter λ. It is noted that for aiding flow (heated cylinder) and to the opposing flow (cooled cylinder), the velocity $f'(\eta)$ increases as f_0 increases but for the temperature profile $\theta(\eta)$ it shows the opposite results. Figure 6 indicates the effects of curvature parameter γ on velocity and temperature profiles for two cases of buoyancy or mixed convection parameter λ. It is observed that the velocity $f'(\eta)$ decreases and the temperature profile $\theta(\eta)$ increases when curvature parameter γ increases in both cases of aiding and opposing flows.

Figure 2 shows the effects of buoyancy or mixed convection parameter λ on velocity and temperature profiles. It is noted that the velocity of fluid increases as λ increases but for the temperature profile it shows the opposite results. Figure 4 shows the effects of Prandtl number Pr on velocity and temperature profiles. As expected, velocity $f'(\eta)$ increases and the temperature $\theta(\eta)$ decreases by increasing Prandtl number. The values of the skin friction coefficient $\frac{1}{2}C_f {Re_x}^{1/2}$ and the local Nusselt number $Nu - x/{Ru_x}^{1/2}$ are given in tables 1 and 2, respectively. Table 1 is made to show the present results in case of aiding flow and compared them with the numerical results reported by Ishak et al. [10], Ramachandran et al. [20], Lok et al. [8] and Hassanien et al. [9]. It is seen from table 2 that the present values of $\frac{1}{2}C_f {Re_x}^{1/2}$ calculated by HAM are in very good agreement with those of numerical results of Ishak et al. [10], Ramachandran et al. [26], Lok et al. [8] and Hassanien et al. [9] Table 2 shows the value of local Nusselt number $Nu - x/{Ru_x}^{1/2}$. It is observed that the skin friction coefficient decrease and the local Nusselt number increases by increasing Pr in assisting flow. During the study of the reliability and effectiveness of the applied method are demonstrated.

An important parameter in fluid flow over a surface is thickness of boundary layer. The boundary layer thickness δ has been defined as the locus of points where the velocity u parallel to the plate reaches %99 of the external velocity U_∞. In other hand, based on $u = Uf'(\eta)$ the $\hat{f}'(\eta) = 0.99$. Finally based on (5) the thickness of boundary layer over vertical slender cylinder defined as follows:

$$\delta \approx \sqrt{2R\eta_{0.99}\sqrt{\frac{\nu x}{U}} + R^2} = \sqrt{2xR\eta_{0.99}Re_x^{-1/2} + R^2} \qquad (۲۴)$$

where $10^3 < Re_x = Ux/\nu < 10^6$ is called the local Reynolds number of the flow along the plate surface [23]. In Equation (24) as shown in Figure 1, R must be subtracted from the obtained value. The equation (24) shows that the boundary-layer thickness is proportional to $\sqrt{\nu}$ and to $\sqrt{x}$. It is clear that δ increases proportionately to $\sqrt{x}$. On the other hand the relative boundary layer thickness δ decreases with increasing Reynolds number, so that in the limiting case of frictionless flow, with $Re \to \infty$, the boundary layer thickness vanishes. As a result of this discuss, for example in, $f_0 = 0$ and $Pr = 1, Pr = 1, \lambda = 1$, the $\eta_{0.99} = 2.91$, and the the thickness for $R = 1, Re_x = 10^3$ can be calculatetd by: $\sqrt{(0.06x + 1)} - 1$.

To show the convergency BFC method (Bessel functions collocation) for solving the equations (6), we have presented the $\| Res(x) \|^2$ defined as follows:

$$||Res(x)||^2 = \int_0^L |Res(x)|^2 dx. \qquad (۲۵)$$

Figure 6-8 show the graphs of the convergency rate for solving the equations (6) for different parameters and several N. These figures show that by increasing the N, the residual tends to zero.

Table ۱. Variation of the skin friction coefficient $f(\eta)''(0)$ with $f_0 = 0, \lambda = 1$ and $\gamma = 0$

Pr	presented method	HAM [32]	shooting	Ishak et al.[10]
0.7	1.706339	1.70634	1.70632	1.7063
1.0	1.675462	1.67540	1.67541	1.6754
7.0	1.517902	1.51790	1.51790	1.5179
10	1.492826	1.49244	1.49282	1.4928
20	1.448594	1.44859	1.44853	1.4485

Table 2. Variation of the skin friction coefficient $\theta'(0)$ with $f_0 = 0, \lambda = 1$ and $\gamma = 0$

Pr	presented method	HAM [32]	shooting	Ishak et al.[10]
0.7	0.764069	0.76400	0.76407	0.7641
1.0	0.870788	0.87051	0.87080	0.8708
7.0	1.722384	1.72124	1.72238	1.7224
10	1.944631	1.94475	1.94462	1.9446
20	2.457606	2.45629	2.45760	2.4576

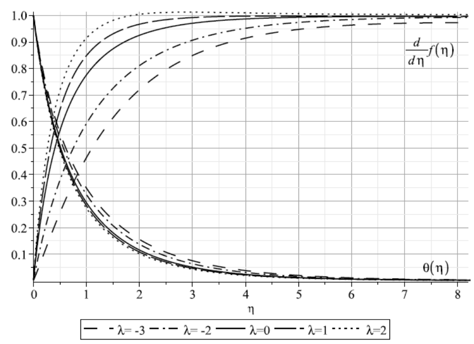

Figure 2. Graph of the approximation function of $f'(\eta)$ and $\theta(\eta)$ by $N = 30$ for several λ and $f_0 = 0.5, \gamma = 1, Pr = 1$

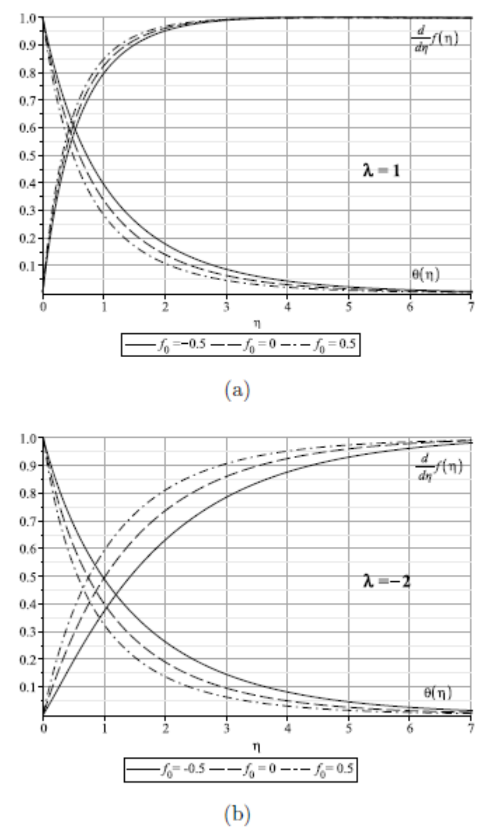

Figure 3. Graph of the approximation function of $f'(\eta)$ and $\theta(\eta)$ by $N = 30$ for several f_0 and $\gamma = 1, Pr = 1$. (a) $\lambda = 1$ and (b) $\lambda = -2$

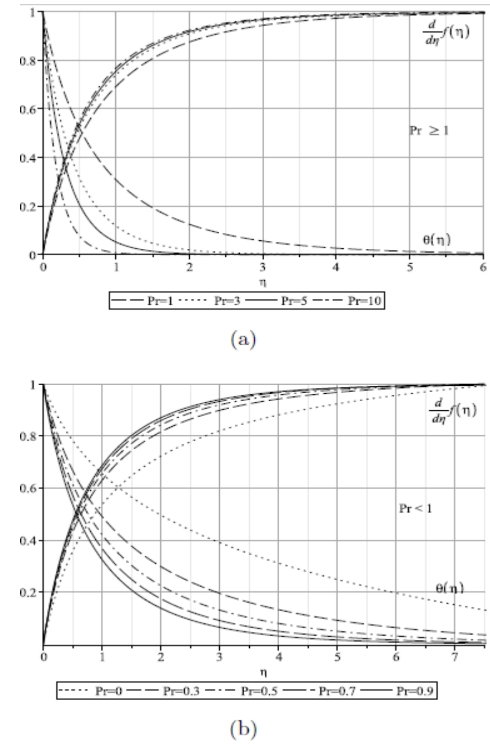

Figure ٤. Graph of the approximation function of $f'(\eta)$ and $\theta(\eta)$ by $N = 30$ for several Pr and $\gamma = 1, \lambda = -2, f_0 = 0.5$. (a) $Pr > 1$ and (b) $Pr < 1$

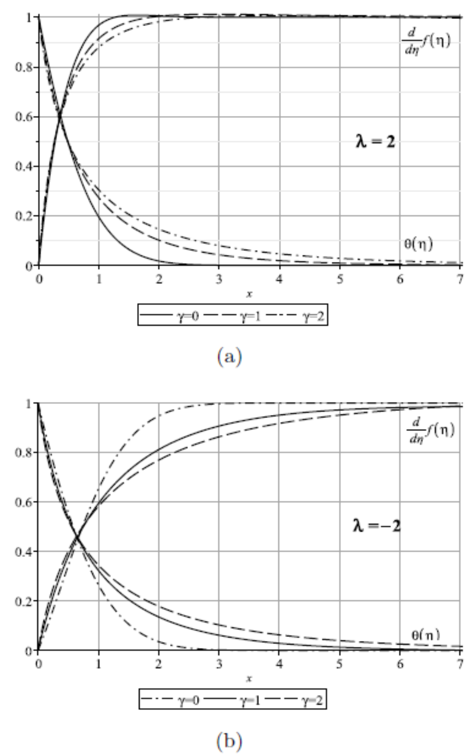

Figure ٥. Graph of the approximation function of $f'(\eta)$ and $\theta(\eta)$ by $N = 30$ for several γ and $f_0 = 0.5, Pr = 1$. (a) $\lambda = 2$ and (b) $\lambda = -2$

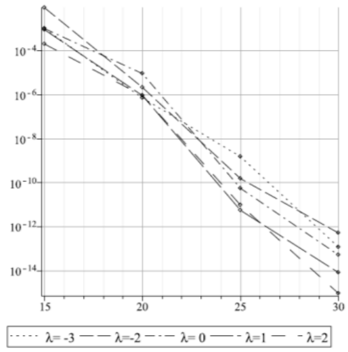

$\| Res_1(x) \|^2$

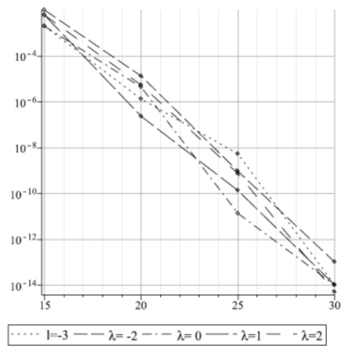

$\| Res_2(x) \|^2$

Figure ٦. Logarithmic graph of the $\| Res_i(x) \|^2$ for $i = 1,2$, several N, several λ and $f_0 = 0.5$, $Pr = 1$

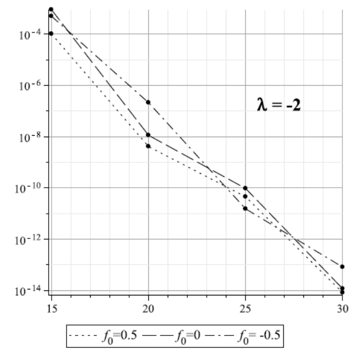

[$\| Res_1(x) \|^2$]

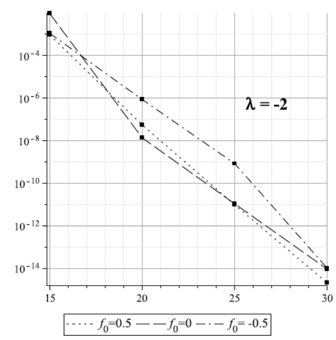

[$\| Res_2(x) \|^2$]

Figure 8. Logarithmic graph of the $\| Res_i(x) \|^2$ for $i = 1,2$, several N, several f_0 and $\lambda = -2$, $Pr = 1$, $\gamma = 1$

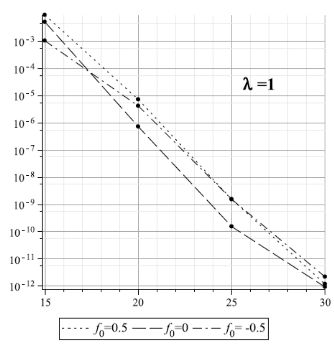

[$\| Res_1(x) \|^2$]

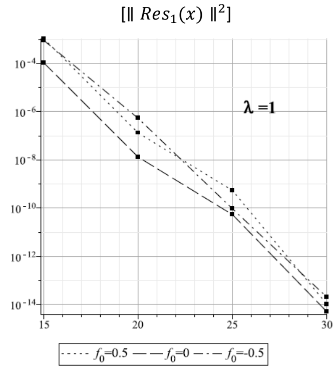

[$\| Res_2(x) \|^2$]

Figure ٧. Logarithmic graph of the $\| Res_i(x) \|^2$ for $i = 1,2$, several N, several f_0 and $\lambda = 1$, $Pr = 1$, $\gamma = 1$

7. Conclusions

The mixed convection boundary layer flow about a vertical slender cylinder in an incompressible viscous fluid is studied. A Spectral solution for the governing equations was obtained that allows the computation of the velocity profile $f'(\eta)$, the temperature profile $\theta(\eta)$, the skin friction coefficient $\frac{1}{2}C_f {Re_x}^{1/2}$ and the local Nusselt number $Nu - x/{Ru_x}^{1/2}$ for various values of the physical parameters curvature parameter γ, buoyancy or mixed convection parameter λ, Prandtl number Pr and f_0. The following observations have been made:

1. The increase in the Prandtl number Pr decreases the skin friction coefficient $\frac{1}{2}C_f {Re_x}^{1/2}$ and increases the local Nusselt number $Nu - x/{Ru_x}^{1/2}$. Also, velocity $f'(\eta)$ increases and the temperature $\theta(\eta)$ decreases by increasing Prandtl number.
2. The velocity $f'(\eta)$ increases and the temperature $\theta(\eta)$ decreases by increasing buoyancy or mixed convection parameter λ.
3. The velocity $f'(\eta)$ decreases and the temperature $\theta(\eta)$ increases by increasing curvature parameter γ.
4. The velocity $f'(\eta)$ increases and the temperature $\theta(\eta)$ decreases by increasing f_0.

Besides, in this work, we introduce a new Spectral-collocation method based on Bessel functions of the first kind to solve equations and system of equations with conditions in the infinite. We solved Eqs. (6) and obtained their solutions with well accuracy and convergence rate, as the obtained results show the applicability and usefulness this method for solving the like these equations.

References

[1] M. Kumari, G. Nath, Mixed convection boundary layer flow over a thin vertical cylinder with localized injection/suction and cooling/heating, I. J. Heat Mass Trans. 47 (2004) 969–976.

[2] T. Aziz, F. Mahomed, Reductions and solutions for the unsteady flow of a fourth grade fluid on a porous plate, Appl. Math. and Comput. 219 (2013) 9187–9195.

[3] A. Aziz, T. Aziz, Mhd flow of a third grade fluid in a porous half space with plate suction or injection: An analytical approach, Appl. Math. and Comput. 218 (2012) 10443–10453.

[4] T. Chen, B. Armaly, Mixed convection in external flow, in: S. Kakac, R.K. Shah, W. Aung, Handbook of Single-Phase Convective Heat Transfer, Wiley, New York, 1987.

[5] K. Vajravelu, K. Prasad, S. Santhi, Axisymmetric magneto-hydrodynamic (mhd) flow and heat transfer at a non-isothermal stretching cylinder, Appl. Math. and Comput. 219 (2012) 3993–4005.

[6] O. Aydin, A. Kaya, Mhd-mixed convection from a vertical slender cylinder, Commun. Nonlinear Sci. Numer. Simulat. 16 (2011) 1863–1873.

[7] H. K. Kuiken, Axisymmetric free convection boundary layer flow past slender bodies, I. J. Heat Mass Trans. 11 (1968) 1141–1153.

[8] Y. Lok, N. Amin, I. Pop, Unsteady mixed convection flow of a micropolar fluid near the stagnation point on a vertical surface, I. J. Thermal Sci. 45 (2006) 1149–1157.

[9] I. A. Hassanien, R. S. R. Gorla, Combined forced and free convection in stagnation flows of micropolar fluids over vertical non-isothermal surfaces, Int. J. Engng Sci. 28 (1990) 783–792.

[10] I. P. A. Ishak, R. Nazar, The effects of transpiration on the boundary layer flow and heat transfer over a vertical slender cylinder, I. J. Non-Linear Mechanics 42 (2007) 1010–1017.

[11] S. Aliabadi, C. Bigler, E. Yilmaz, S. Palle, B. Soni, Hybrid finite element/volume method for 3d incompressible flows with heat transfer, I. J. Comput. Fluid Dynamics 25.

[12] Q. M. Al-Mdallal, A numerical study of initial flow past a circular cylinder with combined streamwise and transverse oscillations, Comput. Fluids 63.

[13] E. Yilmaz, S. Aliabadi, Surface conformed linear mesh and data subdivision technique for large-scale flow simulation and visualization in variable intensity computational environment, Comput. Fluids In Press.

[14] C. Wang, Exact solutions of the steady-state navier-stokes equations, Annu. Rev. Fluid Mech. 23 (1991) 159–177.

[15] H. Schlichting, K. Gersten, Boundary layer theory. 6th ed, Oxford, New York, 1979.

[16] J. Shen, T. Tang, L. L. Wang, Spectral Methods Algorithms, Analysics And Applicattions, first edition, Springer, 2001.

[17] D. Gottlieb, S. A. Orszag, Numerical Analysis of Spectral Methods: Theory and Applications, SIAM, Philadelphia, Pennsylvania, 1977.

[18] K. Parand, M. Nikarya, ANew numerical method based on Generalized Bessel function to solve nonlinear Abel fractional differential equation of the first kind, Nonlinear Engin. 2018 (2010) 1096–1108.

[19] K. Parand, M. Nikarya, J. A. Rad, F. Baharifard, A new reliable numerical algorithm based on the first kind of bessel functions to solve prandtl blasius laminar viscous flow over a semi-infinite flat plate, Zeitsc. fur Naturf. A 67a (2012) 665–673.

[20] K. Pranad, M.Nikarya, Application of Bessel functions and Jacobian free Newton method to solve time-fractional Burger equation, Nonlinear Engin. 8 (2019) 688-694.

[21] S. Yuzbasi, M. Sezer, An improved bessel collocation method with a residual error function to solve a class of lane-emden differential equations, Math. Comput. Model. 57 (2013) 1298–1311.

[22] S. Yuzbasi, N. Sahin, M.Sezer, Bessel polynomial solutions of high-order linear volterra integro-differential equations, Comput. Math. with Appl. 62 (2011) 1940–1956.

[23] M. M. Rashidi, Buoyancy effects on forced convection along a vertical cylinder, J. Heat Transfer 97 (1975) 198–203.

[24] A. Ishak, R. Nazar, I. Pop, Dual solutions in mixed convection flow near a stagnation point on a vertical porous plate, Int. J. Therm. Sci. 47 (2008) 417–422.

[25] T. Mahmood, J. Merkin, Similarity solutions in axisymmetric mixedconvection boundary-layer flow, J. Eng. Math. 22 (1998)) 73–92.

[26] N. Ramachandran, T. Chen, B. Armaly, Mixed convection in stagnation flows adjacent to a vertical surfaces, ASME J. Heat Transfer 110 (788) 373–377.

[27] G. Watson, A treatise on the theory of Bessel Functions, 2nd edition, Cambridge University Press, Cambridge (England), 1967.

[28] W. W. Bell, Special Functions For Scientists And Engineers, Published simultaneously in Canada by D. Van Nostrand Company, (Canada), Ltd, 1967.

[29] E. Kreyszig, Introductory functional analysis with applications, John Wiley, New York, 2000.

[30] N. Vaziria, M. J. Cherna, , A. Borthwickc, A pseudospectral σ-transformation model of solitary waves in a tank with uneven bed, Comput. Fluids 49.

[31] K. Parand, M. Nikarya, A Novel Method to Solve Nonlinear Klein-Gordon Equation Arising in Quantum Field Theory Based on Bessel Functions and Jacobian Free Newton-Krylov Sub-Space Methods, Commun. Theor. Phys. 69 (2018) 637.

[32] J. Rad, K. Parand, S. Abbasbandy, D. Modarrespoor, Analytical solution of the transpiration on the boundary layer flow and heat transfer over a vertical slender cylinder, appear in Quaest. Math. In Press.